Diameter-selective dispersion of single-walled carbon nanotubes using a water-soluble, biocompatible polymer†

Hui Yang,*[ab] Shiunchin C. Wang,[a] Philippe Mercier[a] and Daniel L. Akins*[a]

Received (in Cambridge, UK) 9th November 2005, Accepted 9th February 2006
First published as an Advance Article on the web 22nd February 2006
DOI: 10.1039/b515896f

One-step diameter-selective dispersion of HiPco single-walled carbon nanotubes has been accomplished through noncovalent complexation of the nanotubes with a water-soluble, biocompatible polymer chitosan at room temperature.

Single-walled carbon nanotubes (SWNTs) have attracted enormous attention because of their highly unusual structural, mechanical and electrical properties. Indeed, their properties have made them attractive candidates for many important applications.[1] A number of challenges, however, must be overcome before SWNTs can be exploited for most of the envisioned applications. These challenges include high-yield synthesis; the ability to isolate SWNTs of particular diameters and chiralities, to a high degree of precision; and development of methods for physically manipulating and chemically processing individual nanotubes or their composites.

Efforts aimed at high synthesis yields of SWNTs with controlled diameters and chiralities have centered on controlled CVD synthesis using metal nanoparticle catalysts of specific diameters and narrow diameter distribution.[2a] This approach has recently been augmented by radiofrequency excitation of the carbon source molecules, promoting CVD synthesis of a narrower population of nanotube types.[2b]

A general approach to acquiring SWNTs of selected diameters and chiralities would appear to be post synthesis isolation of SWNTs that have the desired values for the parameters, or other characteristics, such as semiconductor *versus* metallic nature, that might be exploited in a particular application. Indeed, although synthesizing and isolating a collection of tubes based on chirality would be the ideal, the ability to collect tubes of a narrow diameter distribution would be quite useful, since such tubes would have a limited range of possible chiralities. In fact, diameter selectivity is a convenient avenue to follow since small-diameter SWNTs, because of enhanced surface energy, can be expected to readily react with appropriate reagents,[3] as well as to form complexes *via* noncovalent wrapping by polymers[4] and other agents such as peptides.[5] Additionally, metallic *versus* semiconducting SWNT separation would be useful and has been recently reported, resulting from physisorption of octadecylamine and 1-octylamine[6] on the sidewalls of SWNTs; such separation of nanotube types is likely due to the selective reactivity of different types of tubes.[7] Additionally, the separation of SWNTs as a result of their metallic or semiconducting character has been accomplished through dielectrophoretic techniques;[8] where agents such as DNA,[9] porphyrin,[10] or bromine ions,[11] have been effective.

It is to be noted that a number of surfactants and polymers have been identified that create dispersions of SWNTs in various media. However, the formation of dispersions in aqueous systems that contain SWNTs that are essentially monodisperse in terms of diameter or chirality represents capabilities that have not yet been attained. In this Communication, we show that the water-soluble and biocompatible chitosan polymer, containing amine and hydroxyl pendent groups, noncovalently wraps HiPco SWNTs resulting in the dispersion and precipitative separation (not requiring centrifugation) of SWNTs based on nanotube diameter. The chemical structure of chitosan (also referred to hereinafter as CHI) can be seen in Figure SI1 of the Supplementary Information (SI). The details of the dispersion, separation and characterization procedures are described in the SI.

Fig. 1 is a comparison of UV-Vis absorption spectra of 0.1 mg/mL SWNTs suspended in sodium dodecylbenzene sulfonate (SDBS) and CHI. Well-resolved and narrow peaks are attributable to interband transitions between van Hove singularities in the density of states (DOS) of individual SWNTs, indicating the presence of SWNTs as individual and/or very small bundles.[12] Generally, without centrifugation, SWNT samples that are dispersed through use of a coating agent exhibit absorption spectra that have broadened peaks, indicating the presence of nanotubes of a range of diameters, nanotubes that are bundled together (possibly in the form of ropes), as well as nanotubes

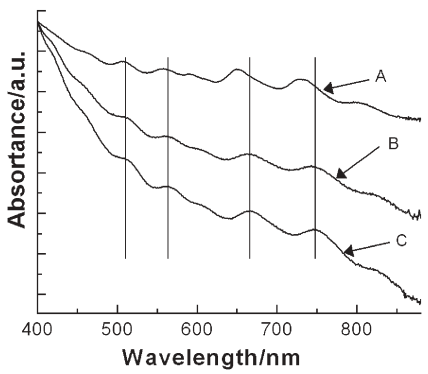

Fig. 1 UV-Vis absorption spectra of 0.1 mg/mL SWNTs suspended after 2 h centrifugation at 29,000 g: (A) suspension in SDBS solution and (B) in CHI solution. Also provided is the spectrum for the CHI system before centrifugation (C).

[a]*Department of Chemistry, The City College of The City University of New York, New York 10031, USA. E-mail: akins@sci.ccny.cuny.edu*
[b]*State Key Lab of Transducer Technology, Shanghai Institute of Microsystem and Information Technology, Chinese Academy of Sciences, Shanghai 200050, China. E-mail: hyang@mail.sim.ac.cn; Fax: +1 212 650 6848*

† Electronic supplementary information (ESI) available: Experimental section. See DOI: 10.1039/b515896f

whose individual transitions frequencies are affected by intermolecular interaction.[12] For such a system, after centrifugation, absorption spectra of SWNTs contained in the supernatant are often found to exhibit sharper peaks, resulting from interband transitions for isolated nanotubes and a decrease in intermolecular interactions. However, for CHI-dispersed SWNTs, no obvious changes in the absorption band widths, before or after 2 h centrifugation, are evident, suggesting, effectively, complete dispersion even before centrifugation. However, we observed a small red-shift in all absorption bands (for both metallic and semiconducting bands) of CHI-dispersed SWNTS as compared to other polymers that have been used to disperse SWNTs,[4] suggesting a nondiscriminative interaction of CHI with both metallic and semiconducting SWNTs.

It is to be noted that once we dispersed SWNTs in CHI aqueous solution, a quantity of black powder spontaneously (overnight) precipitated from dispersion, with the resultant supernatant being homogeneous, stable and of dark color (see Figure SI2). The precipitate could not be redispersed using CHI solution in combination with centrifugation and heating, suggesting a robust method of forming stable SWNTs in solution.

It is known that 632.8 nm radiation, to some degree, excites Raman spectra of both semiconducting and metallic HiPco nanotubes, but mostly semiconducting nanotubes. Fig. 2 shows Raman spectra of the raw HiPco SWNT sample, the dispersion of 0.1 mg/mL SWNTs in CHI solution without centrifugation, and the noncentrifuged precipitate. In Fig. 2(A), curves (a), (b) and (c), the G^+ bands at *ca.* 1590 cm^{-1} and the distinctive shoulder peaks at *ca.* 1551 cm^{-1} (*i.e.*, G^- bands) associated with the E_{2g} optical mode of graphite, and characteristic of sp^2 hybridized carbon materials, indicate the presence of SWNTs. Curve (b) of Fig. 2(A) reveals that in the supernatant the G^+ band is narrower and the G^- band has diminished intensity relative to their respective intensities in the raw HiPco sample, curve (a), while, for the precipitate, curve (c), the G^+ band is broader and the G^- band has enhanced intensity compared to the respective band of the raw HiPco sample. These findings suggest that more semiconducting nanotubes exist in the supernatant and more metallic tubes in the precipitate. Furthermore, in the low-frequency radial breathing mode (RBM) region, shown in Fig. 2(B), characteristic vibrations of SWNT are also found. As shown in curve (a) of Fig. 2(B), for the raw HiPco sample, five distinct RBM peaks are found at *ca.* 192, 214, 255, 280 and 292 cm^{-1} (labeled as i, ii, iii, iv and v, respectively), corresponding to calculated nanotube diameters of 1.24, 1.11, 0.92, 0.83 and 0.79 nm, respectively, using the expression $d(nm) = 223.5/(\omega_{RBM}(cm^{-1}) - 12.5)$ as the correlation between diameter d(nm) and RBM frequency.[13] As reported in the literature, RMB bands above *ca.* 240 cm^{-1}, corresponding to smaller diameter nanotubes, are attributable to semiconducting tubes with chiral indices (n,m) of (10,3), (11,1), (9,4), (7,5) and (8,3) nanotubes;[3,8,14] while RBM bands below 240 cm^{-1} are attributable to metallic tubes with indices of (13,4) and (12,3).[3,8,14] For CHI-dispersed SWNTs, however, only two RBM bands at *ca.* 258 and 284 cm^{-1} occur, corresponding to SWNTs having diameters of 0.91 and 0.82 nm, respectively, using the above correlation. These bands are ascribed to semiconducting nanotubes, and indicate an enrichment of small-diameter semiconducting SWNTs in the supernatant. For SWNTs in the precipitate (*i.e.*, curve (c) of Fig. 2), the RBM peaks at *ca.* 292 and 280 cm^{-1}, in the raw sample, are not present and the RBM band at *ca.* 255 cm^{-1} shows a significantly diminished intensity with respect to the band at *ca.* 214 cm^{-1}, attributable to large-diameter metallic nanotubes, which is greatly enhanced. The above observations suggest that smaller diameter semiconducting SWNTs exist in the supernatant, while larger diameter metallic nanotubes are present in the precipitate.

As a check on our determination above, we acquired Raman spectra of samples identical to those above, but using 514.5 nm excitation, which is expected to generate Raman scattering mainly by metallic nanotubes. In Fig. 3(A), curves (a), (b) and (c), the G^+ and G^- bands, indicate the presence of SWNTs. From curve (b) it is hard to decipher whether the G^+ band is broader or narrower than those in either curves (a) or (c). But the G^- band in curve (c) is clearly enhanced relative to the corresponding band in curve (a). We can conclude that with 514.5 nm excitation the metallic nanotube concentration is greater in the precipitate; but our conclusion is not compelling, and likely associated with poor resonance discrimination between tube types when 514.5 nm excitation is used. However, bands in the RBM region provide better insight. In the RBM region in Fig. 3(B), for raw HiPco SWNTs (curve (a)), there are four distinct peaks located at *ca.* 185, 208, 248 and 264 cm^{-1} (labeled as i, ii, iii and iv, respectively), corresponding to the nanotube diameters of 1.30, 1.14, 0.94 and 0.89 nm, respectively, upon using the correlation described earlier. The RBM bands at 248 and 264 cm^{-1} are attributable to metallic

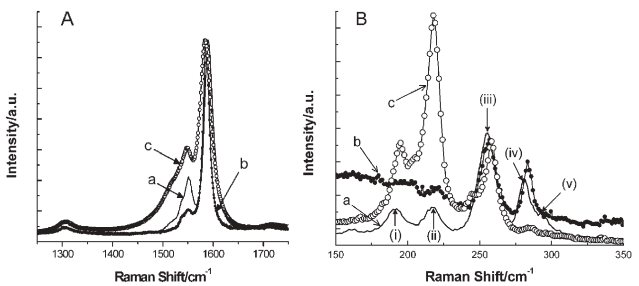

Fig. 2 Part A shows Raman spectra using 632.8 nm excitation in the G^- band region: (a) raw HiPco SWNT sample, (b) dispersion of 0.1 mg/mL SWNTs in chitosan solution without centrifugation, and (c) noncentrifuged precipitate. The spectra in Part A are normalized to the G^+ band feature. Part B shows Raman spectra in the RBM region for the same samples (a), (b) and (c) as above; intensities of curves (b) and (c) have been multiplied by a factor of 2 for presentation purposes.

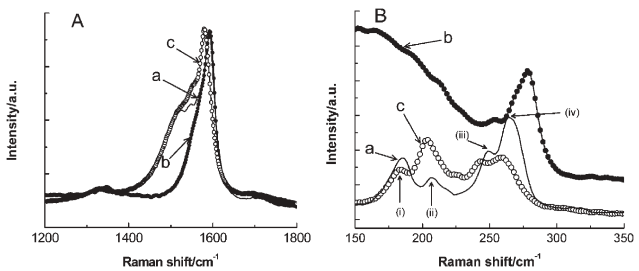

Fig. 3 Part A shows Raman spectra using 514.5 nm excitation in the G-band region of: (a) raw HiPco SWNT sample, (b) dispersion of 0.1 mg/mL SWNTs in chitosan solution without centrifugation, and (c) noncentrifuged precipitate. The spectra in Part A are normalized to the G^+ band feature. Part B shows Raman spectra in the RBM region for the same samples (a), (b) and (c) as above.

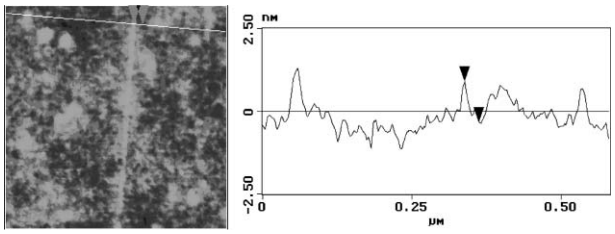

Fig. 4 Tapping mode AFM image of 0.1 mg/mL SWNTs dispersed in 0.5 wt.% chitosan aqueous solution after 2 h centrifugation and coated onto a mica substrate. The left hand panel shows a nearly vertically aligned coated SWNT and chitosan nanoparticles; the line from left to right is the traversal direction that gives the right hand panel information. The right hand panel presents the height analysis.

tubes with (n,m) indices of (12,0) and (9,3),[3,8] respectively, and the band at 185 cm^{-1} has been attributed to semiconducting nanotubes of indices (16,0).[3,8] The RBM band at 208 cm^{-1} is attributed to metallic nanotubes.[8] For CHI-dispersed SWNTs (curve (b)), two RBM bands are found (at *ca.* 265 and 273 cm^{-1}), corresponding to SWNTs having diameters of 0.89 and 0.86 nm, respectively, of which the latter band has been assigned to a (8,5) metallic tube.[8] For the SWNTs in the precipitate (curve (c)), one finds that RBM bands at lower wavenumbers, corresponding to the larger-diameter semiconducting nanotubes, are enhanced and RBM bands at higher wavenumber, due to the smaller-diameter metallic nanotubes, are decreased. It is clear that small-diameter SWNTs are selectively wrapped by polymer, resulting in the larger-diameter nanotubes being found in the precipitate.

For both 632.8 and 514.5 nm excited Raman spectra, the collective conclusion is that small diameter nanotubes, independent of whether they are semiconducting or metallic, are selectively dispersed by CHI, allowing separation of SWNTs based on their diameters.

Fig. 4 provides a typical AFM image of SWNTs dispersed in CHI aqueous solution (after 2 h centrifugation) and coated onto a mica substrate. Additional AFM images are provided in the Supporting Information. The AFM image reveals separated and individual SWNTs wrapped with CHI that have been adsorbed onto mica. These samples have been found to be extremely stable and do not spontaneously rebundle. From the AFM images, the height of the tubes is visualized as approximately 1.22–1.48 nm, and is interpreted as indicating that individual HiPco SWNTs are surrounded by chitosan molecules. It is to be noted that in the AFM images one finds many free chitosan nanoparticles on the mica surface, consistent with chitosan selectively wrapping nanotubes of a limited diameter range or not at all, freeing up unused chitosan to form the nanoparticles.

In conclusion, we have developed a simple, efficient process for the water dispersion and diameter-selective separation of single-walled carbon nanotubes, unlike the other reported approaches in which a repetitive dispersion–centrifugation process is required. "Smaller-diameter" SWNTs are preferentially dispersed and wrapped by chitosan in the aqueous supernatant that results following noncentrifuged precipitation, while "larger-diameter" SWNTs exist in the precipitate.

DLA thanks the NSF-IGERT program under grant DGE-9972892, the NSF-MRSEC program under grant DMR-0213574, the NSF-NSEC program under grant CHE-0117752, and DoD-ARO under Cooperative Agreement DAAD19-01-1-0759 and grant W911NF-04-1-0029.

Notes and references

1 (*a*) P. G. Collins, A. Zettl, H. Bando, A. Thess and R. E. Smalley, *Science*, 1997, **278**, 100; (*b*) A. Bachtold, P. Hadley, T. Nakanishi and C. Dekker, *Science*, 2001, **294**, 1317; (*c*) M. S. Fuhrer, L. Nygard, M. Forero, Y. E. Yoon, M. S. C. Mazzoni, H. J. Choi, J. Ihm, S. G. Louie, A. Zettl and P. L. McEuen, *Science*, 2000, **288**, 494.
2 (*a*) L. An, J. M. Owens, L. E. McNeil and J. Liu, *J. Am. Chem. Soc.*, 2002, **124**, 13688; (*b*) Y. Li, D. Mann, M. Rolandi, W. Kim, A. Ural, S. Hung, A. Javey, J. Cao, D. Wang, E. Yenilmiz, Q. Wang, J. F. Gibbons, Y. Nishi and H. Dai, *Nano Lett.*, 2004, **4**, 317.
3 S. Banerjee and S. S. Wong, *Nano Lett.*, 2004, **4**, 1445.
4 (*a*) S. M. Keogh, T. G. Hedderman, E. Gregan, G. Farrell, G. Chambers and H. Byne, *J. Phys. Chem. B*, 2004, **108**, 6233; (*b*) A. B. Dalton, C. Stephan, J. N. Coleman, B. McCarthy, P. M. Ajayan, S. Lefrant, P. Bernier, W. J. Blau and H. J. Byrne, *J. Phys. Chem. B*, 2000, **104**, 10012; (*c*) A. Star, J. F. Stoddart, D. Steuerman, M. Diehl, A. Boukai, E. W. Wong, X. Yang, S. W. Chung, H. Choi and J. R. Heath, *Angew. Chem., Int. Ed.*, 2001, **40**, 1721.
5 A. Ortiz-Acevedo, H. Xie, V. Zorbas, W. M. Sampson, A. B. Dalton, R. H. Baughman, R. K. Draper, I. H. Musselman and G. R. Dieckmann, *J. Am. Chem. Soc.*, 2005, **127**, 9512.
6 (*a*) D. Chattopadhyay, I. Galeska and F. Papadimitrakopoulos, *J. Am. Chem. Soc.*, 2003, **125**, 3370; (*b*) Y. Maeda, S. Kimura, M. Kanda, Y. Hirashima, T. Hasegawa, T. Wakahara, Y. Lian, T. Nakahodo, T. Tsuchiya, T. Akasaka, J. Lu, X. Zhang, Z. Gao, Y. Yu, S. Nagase, S. Kazaoui, N. Minami, T. Shimizu, H. Tokumoto and R. Saito, *J. Am. Chem. Soc.*, 2005, **127**, 10287.
7 M. S. Strano, C. A. Dyke, M. L. Usrey, P. W. Barone, M. J. Allen, H. Shan, C. Kittrell, R. H. Hauge, J. M. Tour and R. E. Smalley, *Science*, 2003, **301**, 1519.
8 R. Krupke, F. Hennrich, H. V. Löhneysen and M. M. Kappes, *Science*, 2003, **301**, 344.
9 M. Zheng, A. Jagota, M. S. Strano, A. P. Santos, P. Barone, S. G. Chou, B. A. Diner, M. S. Dresselhaus, R. S. Mclean, G. B. Onoa, G. G. Samsonidze, E. D. Semke, M. Usrey and D. J. Walls, *Science*, 2003, **302**, 1545.
10 H. Li, B. Zhou, Y. Lin, L. Gu, W. Wang, K. A. S. Fernando, S. Kumar, L. F. Allard and Y. P. Sun, *J. Am. Chem. Soc.*, 2004, **126**, 1014.
11 Z. Chen, X. Du, M. H. Du, C. D. Rancken, H. P. Cheng and A. G. Rinzler, *Nano Lett.*, 2003, **3**, 1245.
12 (*a*) M. F. Islam, E. Rojas, D. M. Bergey, A. T. Johnson and A. G. Yodh, *Nano Lett.*, 2003, **3**, 269; (*b*) V. C. Moore, M. S. Strano, E. H. Haroz, R. H. Hauge, R. E. Smalley, J. Schmidt and Y. Talmon, *Nano Lett.*, 2003, **3**, 1379.
13 S. M. Bachilo, M. S. Strano, C. Kittrell, R. H. Hauge, R. E. Smalley and R. B. Weisman, *Science*, 2002, **298**, 2361.
14 C. A. Dyke and J. M. Tour, *J. Phys. Chem. A*, 2004, **108**, 11151.